# Abrupt GaP/Si hetero-interface using bistepped Si buffer

Y. Ping Wang,[1,a)] J. Stodolna,[2,b)] M. Bahri,[3] J. Kuyyalil,[1,c)] T. Nguyen Thanh,[1,d)] S. Almosni,[1] R. Bernard,[1] R. Tremblay,[1] M. Da Silva,[1] A. Létoublon,[1] T. Rohel,[1] K. Tavernier,[1] L. Largeau,[3] G. Patriarche,[3] A. Le Corre,[1] A. Ponchet,[2] C. Magen,[4] C. Cornet,[1] and O. Durand[1]

[1]*UMR FOTON, CNRS, INSA Rennes, Rennes F-35708, France*
[2]*CEMES-CNRS, Université de Toulouse, 29 rue Jeanne Marvig, BP 94347, 31055 Toulouse Cedex 04, France*
[3]*Laboratoire de Photonique et Nanostructures, CNRS UPR 20, Route de Nozay, Marcoussis 91460, France*
[4]*LMA, INA-ARAID, and Departamento de Física de la Materia Condensada, Universidad de Zaragoza, 50018 Zaragoza, Spain*

(Received 24 July 2015; accepted 29 October 2015; published online 11 November 2015)

We evidence the influence of the quality of the starting Si surface on the III-V/Si interface abruptness and on the formation of defects during the growth of III-V/Si heterogeneous crystal, using high resolution transmission electron microscopy and scanning transmission electron microscopy. GaP layers were grown by molecular beam epitaxy on vicinal Si (001). The strong effect of the Si substrate chemical preparation is first demonstrated by studying structural properties of both Si homoepitaxial layer and GaP/Si heterostructure. It is then shown that choosing adequate chemical preparation conditions and subsequent III-V regrowth conditions enables the quasi-suppression of micro-twins in the epilayer. Finally, the abruptness of GaP/Si interface is found to be very sensitive to the Si chemical preparation and is improved by the use of a bistepped Si buffer prior to III-V overgrowth. © *2015 AIP Publishing LLC*.
[http://dx.doi.org/10.1063/1.4935494]

The heterogeneous epitaxy of III-V semi-conductors on silicon has been widely studied in the context of the monolithic integration of low-cost photonics on silicon. However, the large lattice mismatch between most of the III-V materials and Si leads to a high density of misfit dislocations. To overcome such issues, the growth of quasi-lattice-matched GaP on Si (misfit of 0.37% at room temperature) has been proposed, to be used as an efficient platform allowing subsequent integration of defect-free III-V based heterostructures.[1–4] Nevertheless, crystalline defect, such as anti-phase domains (APD)[5–8] and micro-twins (MT),[9,10] can be generated at the GaP/Si interface. These defects are detrimental to optoelectronic properties of the devices and have to be avoided for long term and stable device performance.[11]

It was shown that the APDs were formed due to polar-on-non polar materials growth and could be partially avoided via double stepped Si (001) surface, realized by using a vicinal Si substrate with a miscut of a few degrees towards the [110] direction.[12–14] Our recent work proved a dramatic annihilation of APDs within the early growth stage.[15] On the other hand, pioneering experiments have attributed the generation of MTs to the 3D nucleation at the early stages of growth.[16] But the impact of the initial Si surface and its chemical preparation was also underlined.[17,18] The Si surface quality at the atomic scale is of great importance for management of both defects during subsequent III-V/Si heterogeneous growth. Furthermore, any intermixing at the interface, leading to a Si-GaP co-doping, should be prevented. The precise control of the III-V/Si interface in term of abruptness and composition is required to obtain efficient tunnel junction for tandem solar cells[19,20] and suitable carrier injection across the interface for integrated photonic devices, as it impacts deeply the band lineups and potentials in such systems. Therefore, the properties of the GaP/Si interface at the atomic scale were investigated recently in several works. With the use of vicinal Si substrates, Grassman *et al.* observed a large step-bunching (over 16 monolayers) and the presence of (113) facets at the GaP/Si interface.[14] Supplie *et al.* found that the formation of the abrupt Si-P heterointerface was kinetically limited.[21] Beyer *et al.* also demonstrated a clear correlation between the Si initial surface, the interfacial properties, and the defect generation.[22] In any cases, obtaining a smooth, contaminant-free Si surface with biatomic steps before the GaP deposition remains one of the key challenges to limit the defect generation at the interface.

In this work, we first study the influence of the silicon chemical preparation on the quality of homoepitaxial Si and heteroepitaxial GaP layers. We then show how the MT formation is related to both silicon surface chemical preparation and III-V overgrowth conditions. We finally point out the relationship between the initial Si surface (chemical preparation, buffer layer) and the quality of the GaP/Si heterointerface.

Here, two methods of silicon substrate surface chemical preparation are compared. The first one is based on the standard Radio Corporation of America (RCA) process[23] and called hereafter the "modified RCA process". The sample is first dipped in the $NH_4OH$-$H_2O_2$-$H_2O$ solution for removing particles and most metallic impurities, then in the

[a)]Author to whom correspondence should be addressed. Electronic mail: yanping.wang@insa-rennes.fr.
[b)]Current address: EDF R&D, Département Matériaux et Mécanique des Composants, Avenue des Renardières, Ecuelles, F-77250 Moret sur Loing, France.
[c)]Current address: Department of Physics, Boston University, 590 Commonwealth Avenue, Boston, MA 02215, USA.
[d)]Current address: European Synchrotron Radiation Facility, B.P. 220, F-38043 Grenoble Cédex, France.

 

HF-$H_2O$ solution and HCl-$H_2O_2$-$H_2O$ solution for oxide removal, and finally in the HF-$H_2O$ solution after an oxidation in UV/$O_3$ atmosphere for residual carbon removal. These steps are repeated 5 times. The second method called hereafter "optimized HF process" consists in a first dipping in HF 1% bath for 90 s, followed by an exposure under UV/$O_3$ for 10 min and a final HF (1%) dipping for 90 s. This process is similar to that reported by Takahagi *et al.* who claimed successful achievement of clean and carbon-free silicon surface[24] and already proved its efficiency for III-V/Si growth.[17,18] Both the Si and GaP crystal growth have been performed in a purposely designed growth cluster composed of a Si-dedicated Ultra-High-Vacuum Chemical Vapor Deposition (UHVCVD) chamber linked under UHV with a III-V dedicated solid source Molecular Beam Epitaxy (MBE) growth chamber.[17] For samples including a Si buffer layer, the homoepitaxial silicon layer has been deposited on the chemically cleaned Si substrate at 800 °C using silane (at a $6 \times 10^{-3}$ Torr pressure) in the UHVCVD growth chamber and transferred under UHV to the MBE growth chamber for GaP overgrowth. For samples without Si buffer, freshly prepared Si substrates are loaded into the MBE chamber, heated at 800 °C for 10 min for dehydrogenation and bisteps formation, and cooled down to GaP growth temperature. All GaP/Si samples have been obtained by the growth of GaP using migration enhanced epitaxy at 350 °C with a starting one (otherwise mentioned) monolayer (ML) of Ga onto Si (001) substrate, misoriented of 6° towards the [110] direction (see Ref. 17 for more details on the growth process). Post-growth analyses have been performed using Scanning Electron Microscopy (SEM), Atomic Force Microscopy (AFM) in contact mode, High Resolution Transmission Electron Microscopy (HRTEM), and High Resolution Scanning TEM (HRSTEM) in bright field (BF) mode and in High Angle Annular Dark Field (HAADF) mode. Here, we outline that each of these techniques allows the observation with an atomic resolution. The HAADF HRSTEM mode is, however, more sensitive to chemical composition and is thus useful for the visualization of the GaP/Si interface. TEM cross-sectional specimens have been prepared by mechanical polishing followed by argon ion milling at low temperature using a Gatan Precision Ion Polishing System equipped with a liquid nitrogen cooling system.

Evaluating the cleanliness of a chemical preparation is not straightforward. Fortunately, the CVD technique is dramatically sensitive to substrate surface contamination. Even low contaminant density results in a rough and holed surface after a homoepitaxial growth. The efficiency of the silicon surface preparation is thus investigated by post-growth surface morphology characterization of silicon buffer layers, using SEM or AFM techniques. As shown in the cross-sectional SEM image (Fig. 1(a)), the modified RCA process followed by 150 nm Si homoepitaxial layer leads to a pitted surface, displaying a flat bottom surface whose depth corresponds to the epitaxial layer thickness. The inclined edges of the groove, showing a constant angle value of 25° with the mean surface, indicate (113) crystal facets. These grooves, also observed in the inserted AFM image, result in a very high r.m.s. surface roughness of 48 nm. This evidences the presence of contaminants at the substrate surface,[25] which prevent any subsequent high-quality epitaxial growth. Fig. 1(b) presents the cross-sectional HRTEM image of a GaP layer grown directly on a Si substrate freshly chemically prepared by the modified RCA process. The GaP/Si interface is quite diffuse with localized bright areas which are attributed to the presence of contaminants at the Si surface. The nature of the contaminants has not

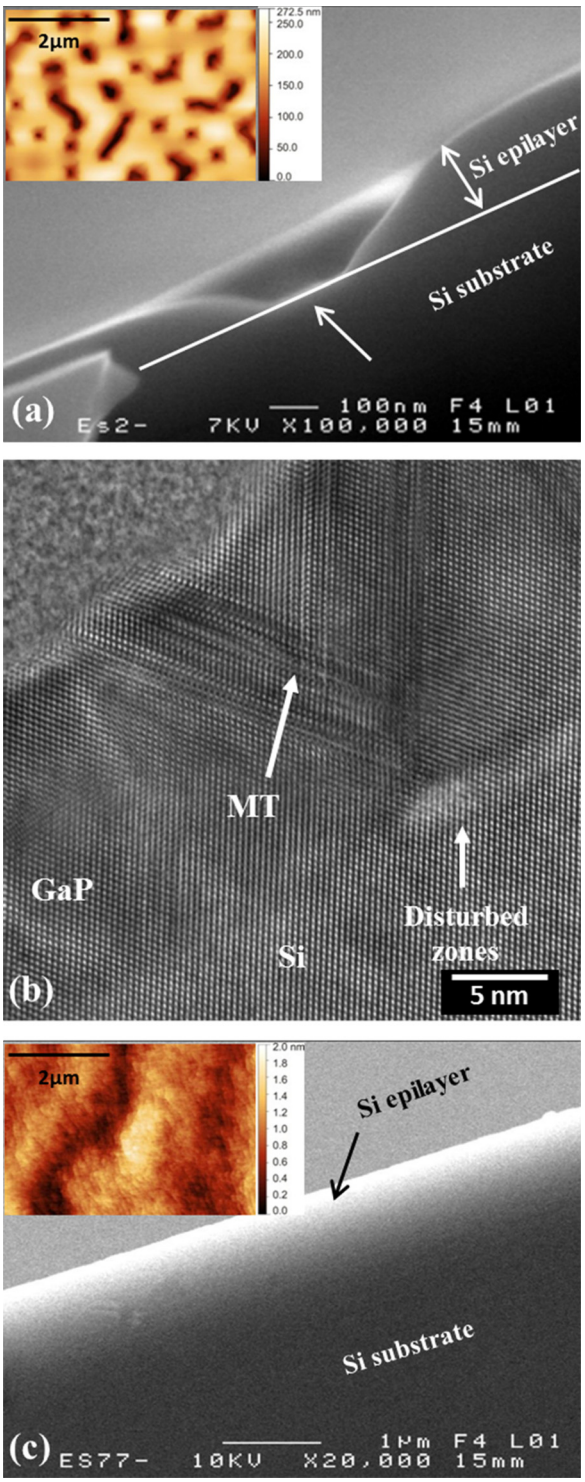


FIG. 1. (a) Cross-sectional SEM image of silicon homoepitaxial layer grown on the Si substrate cleaned by modified RCA process. Insetted AFM image shows high r.m.s. surface roughness (48 nm); (b) HRTEM images of a GaP epilayer grown on the Si substrate cleaned by modified RCA process; (c) cross-sectional SEM image of silicon homoepitaxial layer grown on the Si substrate cleaned by optimized HF cleaning process. The r.m.s. roughness measured on insetted AFM image is about 0.3 nm.

been determined, but is usually assumed to be carbon or oxygen atoms.[26] This assumption is supported by various observations made at different scales on samples with different chemical preparations and different III-V regrowth conditions, but not shown here for clarity. In this situation, large packets of MTs are generated from these disturbed zones and emerge to the GaP surface, which has been also observed on different parts of different samples. The optimized HF cleaning process is then used before Si homoepitaxy, leading to a smooth Si epilayer without any detectable defects (pits, holes, and grooves) and a r.m.s. roughness around 0.3 nm, as shown by cross-sectional SEM and AFM images (Fig. 1(c)). This indicates that the substrate surface was efficiently cleaned before Si growth. Note that the modified RCA chemical preparation is not questioned here, as it has already largely proved its efficiency. We attribute these observations to the numerous wet chemical steps used in the modified RCA process. This likely increases the exposure of the silicon surface to non-intentional contaminations, if the purity of the chemical solutions and the chemical environment is not perfectly controlled. The main advantage of the optimized HF cleaning process is therefore the limitation of the silicon substrate exposure to chemical solutions.

Fig. 2 presents the cross-sectional HRSTEM-BF images of GaP layers grown on the Si surface prepared by the optimized HF cleaning process. The only difference between the two samples is the initial Ga coverage of the silicon surface (1 ML for the first sample in Fig. 2(a) and 0.75 ML for the second sample in Fig. 2(b)). In these samples, the interface is clearly more abrupt than the one presented in Fig. 1(b) whose Si surface is prepared by the modified RCA process. The chemical preparation has therefore a great influence on the interface abruptness. Moreover, most of the large bunches of MTs depicted in Fig. 1(b) have been suppressed. This has been confirmed with large-scale observation and in different parts of the sample. Several single isolated MTs are generated for the sample with an initial 1 ML Ga coverage, as shown in Fig. 2(a). However, their nature is clearly different from the large MT bunches. Fig. 2(b) shows the cross-sectional HRSTEM-BF image of the GaP layer grown under slightly different growth conditions (with 0.75 ML Ga coverage). No MT is observed anymore, which is also confirmed by observations on larger scales in different parts of the sample. This observation is in good agreement with what has been observed by Volz *et al.*, who already showed that an excessive initial Ga coverage significantly increased the number of generated defects.[27] A more statistical analysis carried out by X-ray diffraction reported elsewhere[15] showed that the recently optimized growth conditions permit reducing the volume fraction of MTs in the whole GaP layer below 1%, the limit of detection of our XRD setup. With these growth conditions, the TEM imaging at large field of view[15] allows to give an estimation of the linear density of MTs as low as 5 MTs/$\mu$m. We therefore conclude that the formation of the single MTs is not related to the presence of residual contaminants, but more likely to the III-V overgrowth conditions (Ga exposure, growth temperature, etc.), and thus can be avoided with a careful optimization of the III-V overgrowth.

Cross-sectional HRSTEM-HAADF imaging has been carried out, allowing Z contrast with atomic resolution, to study more accurately the GaP/Si interface. Fig. 3(a) shows the HAADF image of a GaP layer directly deposited on the Si surface prepared by the modified RCA process. The GaP/Si interface is very diffuse. Conventional TEM observations also revealed a large density of crystalline defects. As shown in Fig. 3(b) and already commented above, the interface for the sample with GaP grown on the Si substrate cleaned by optimized HF process is much sharper. Fig. 3(c) shows the GaP/Si interface when a Si buffer is grown prior to the GaP overgrowth. The interface is clearly sharper and displays an appearing periodicity of 6–7 atoms, in agreement with the theoretical value of 6.7 atoms per terrace (between two step edges), in the case of bistepped Si substrate misoriented of 6° towards [110]. Still, these findings have been checked on different parts of the sample, and conclusions remain.

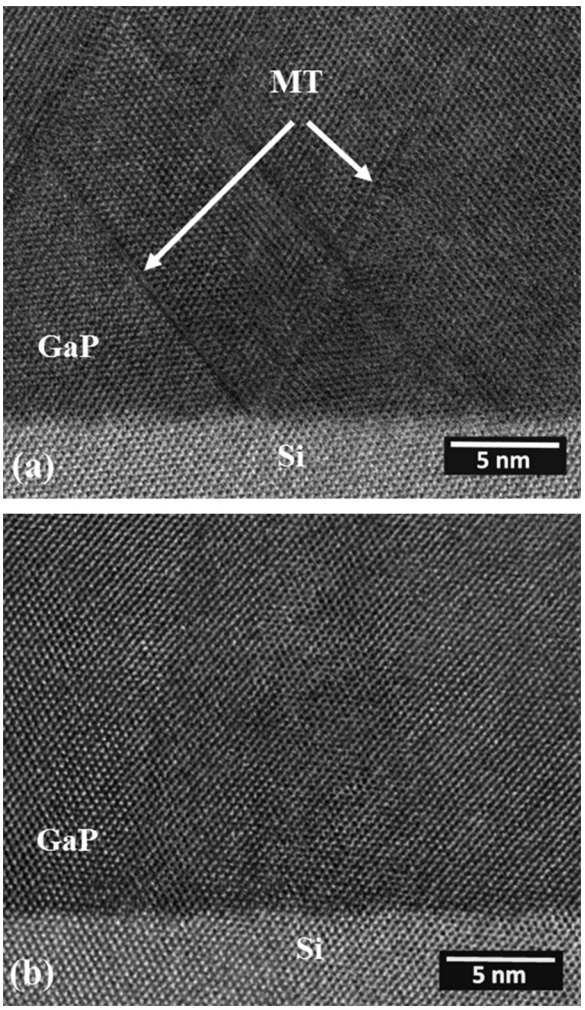


FIG. 2. Cross-sectional HRSTEM-BF image of GaP epilayer grown on the optimized HF process cleaned Si substrate with an initial (a) 1 ML Ga coverage and (b) 0.75 ML Ga coverage on the silicon surface.

To confirm the bistep formation, Fig. 4 shows the cross profile analysis of the Reflection High-Energy Electron Diffraction (RHEED) pattern observed during the homoepitaxial Si buffer growth by UHVCVD on a 6°-off silicon substrate, presenting a 2 × n pattern. The 2× pattern is observed when the electron beam is parallel to the [110] direction (perpendicular to the step edges) and the ×n pattern is observed in the [1–10] direction (parallel to the step edges), n being the number of atoms on the terrace along the [110]

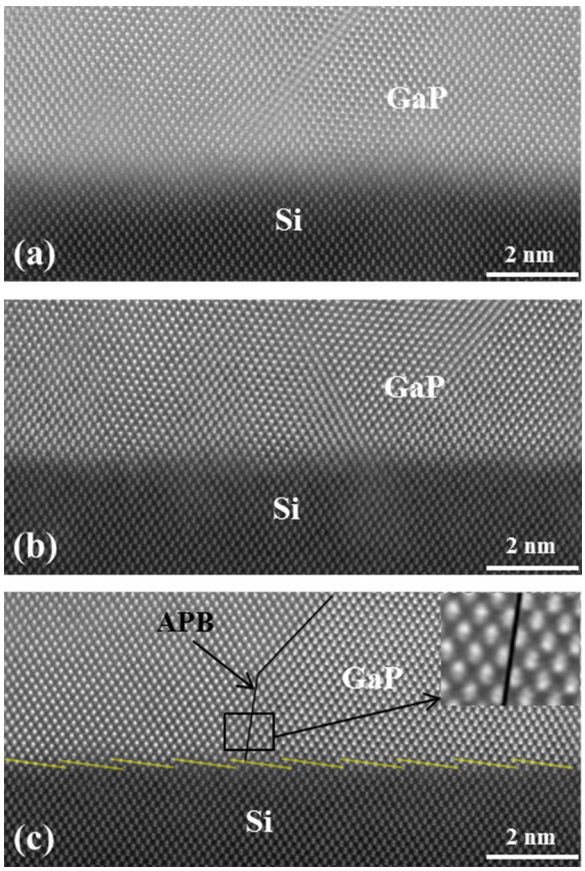


FIG. 3. Cross-sectional HRSTEM-HAADF images of (a) GaP epilayer directly grown on the modified RCA process prepared Si surface, (b) GaP epilayer directly grown on the optimized HF process prepared Si surface, and (c) GaP epilayer grown on the optimized HF process prepared Si surface, with a homoepitaxial Si buffer layer prior to the GaP growth. Inset is the magnified image of the enclosed zone, evidencing the inversion of Ga-P dumbbells from one side of the APB to the other side.

direction. This was already widely discussed in the literature.[30] The mean value of n can be roughly calculated with $n = L/l$, where L and l represent the diffraction spots interval, respectively, from the surface lattice and the terrace length along [110] direction.[31] The average values of L and l are measured to be 57.4 and 8.1 (arbitrary units), respectively, giving rise to $n \sim 7$ (corresponding to a terrace length of 2.69 nm). This is consistent with the theoretical terrace length (2.58 nm) on a bistepped vicinal surface with a 6° miscut and confirms the previous HRSTEM-HAADF observations. This $2 \times n$ RHEED pattern has not been clearly observed during the simple 10 min annealing at 800 °C used for samples without buffer layers. The Si buffer layer is therefore expected to increase the biatomic step coverage of the surface. Interestingly, despite the apparently observed double-stepped GaP/Si interface, antiphase boundaries (APBs) are still visible in the GaP/Si sample with a Si buffer (see the black solid line in Fig. 3(c) and corresponding inset). APBs can be evidenced by specific contrasts in atomic resolved images, as reported, for instance, by Narayanan[28] using HRTEM and Bayer[29] using HRSTEM HAADF technique. Here, as in Ref. 29, the inserted magnified image shows clearly the inversion of the Ga-P dumbbells from one side of the APB to the other side. Note that several antiphase domains can also be evidenced on other samples of Figs. 3(a) and 3(b). This confirms the importance of controlling the initial group III or group V coverage of the Si surface before any III-V growth, even if performed on a bistepped Si surface.

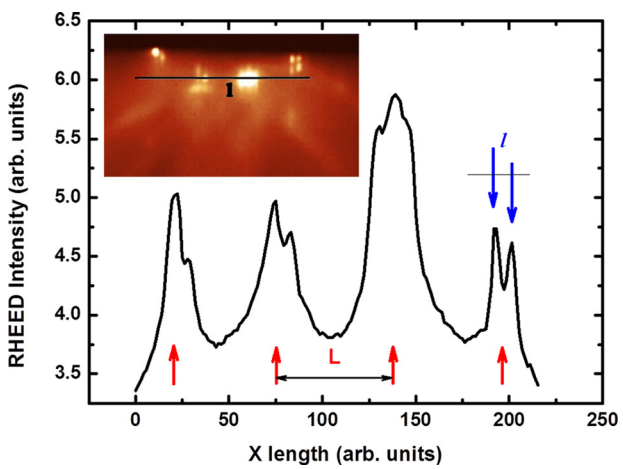


FIG. 4. The RHEED pattern measured during homoepitaxial Si growth by UHVCVD on 6°-off Si (100) substrate and the cross profile analysis. Red upward pointing arrows indicate the diffraction spots from the surface lattice along [110] direction and blue downward pointing arrows indicate the diffraction spots from the steps length. Calculation from average l and L gives $n = L/l \sim 7$. Inset shows the RHEED pattern in which the profile is extracted.

In summary, we have evidenced the influence of the starting Si surface on the GaP/Si interface abruptness and on the generation of defects during GaP/Si heterogeneous crystal growth. While the presence of contaminants introduced by the chemical preparation of the Si substrate leads to large MT stacks in the III-V epilayer, single isolated MTs have to be related to growth conditions and can be suppressed with adapted III-V growth conditions. Finally, the abruptness of GaP/Si interface is found to be very sensitive to the Si chemical preparation and is improved by the use of a bistepped Si buffer prior to III-V overgrowth, even though it does not guarantee the absence of antiphase boundaries.

This work was supported by the French National Research Agency Projects MENHIRS (Grant No. ANR-2011-PRGE-007-01), OPTOSI (Grant No. 12-BS03-002) and ANTIPODE (Grant No. 14-CE26-0014-01). The research leading to these results has received funding from the European Union Seventh Framework Program under Grant Agreement No. 312483-ESTEEM2 (Integrated Infrastructure Initiative–I3). Y. Ping Wang wishes to thank the Chinese scholarship council (CSC) for financial support.

[1]B. Kunert, K. Volz, J. Koch, and W. Stolz, Appl. Phys. Lett. **88**, 182108 (2006).
[2]K. Samonji, H. Yonezu, Y. Takagi, K. Iwaki, N. Ohshima, J. K. Shin, and K. Pak, Appl. Phys. Lett. **69**, 100 (1996).
[3]C. Robert, A. Bondi, T. N. Thanh, J. Even, C. Cornet, O. Durand, J. P. Burin, J. M. Jancu, W. Guo, A. Létoublon, H. Folliot, S. Boyer-Richard, M. Perrin, N. Chevalier, O. Dehaese, K. Tavernier, S. Loualiche, and A. Le Corre, Appl. Phys. Lett. **98**, 251110 (2011).
[4]H. Yonezu, Y. Furukawa, and A. Wakahara, J. Cryst. Growth **310**, 4757 (2008).
[5]H. Kroemer, J. Cryst. Growth **81**, 193 (1987).

[6]A. Létoublon, W. Guo, C. Cornet, A. Boulle, M. Véron, A. Bondi, O. Durand, T. Rohel, O. Dehaese, N. Chevalier, N. Bertru, and A. L. Corre, J. Cryst. Growth **323**, 409 (2011).
[7]W. Guo, A. Bondi, C. Cornet, A. Létoublon, O. Durand, T. Rohel, S. Boyer-Richard, N. Bertru, S. Loualiche, J. Even, and A. L. Corre, Appl. Surf. Sci. **258**, 2808 (2012).
[8]A. C. Lin, M. M. Fejer, and J. S. Harris, J. Cryst. Growth **363**, 258 (2013).
[9]G. A. Devenyi, S. Y. Woo, S. Ghanad-Tavakoli, R. A. Hughes, R. N. Kleiman, G. A. Botton, and J. S. Preston, J. Appl. Phys. **110**, 124316 (2011).
[10]T. Nguyen Thanh, C. Robert, E. Giudicelli, A. Létoublon, C. Cornet, A. Ponchet, T. Rohel, A. Balocchi, J. S. Micha, M. Perrin, S. Loualiche, X. Marie, N. Bertru, O. Durand, and A. L. Corre, J. Cryst. Growth **378**, 25 (2013).
[11]E. Tea, J. Vidal, L. Pedesseau, C. Cornet, J.-M. Jancu, J. Even, S. Laribi, J.-F. Guillemoles, and O. Durand, J. Appl. Phys. **115**, 063502 (2014).
[12]S. F. Fang, K. Adomi, S. Iyer, H. Morkoç, H. Zabel, C. Choi, and N. Otsuka, J. Appl. Phys. **68**, R31 (1990).
[13]T. J. Grassman, M. R. Brenner, S. Rajagopalan, R. Unocic, R. Dehoff, M. Mills, H. Fraser, and S. A. Ringel, Appl. Phys. Lett. **94**, 232106 (2009).
[14]T. J. Grassman, J. A. Carlin, B. Galiana, L.-M. Yang, F. Yang, M. J. Mills, and S. A. Ringel, Appl. Phys. Lett. **102**, 142102 (2013).
[15]Y. Ping Wang, A. Letoublon, T. Nguyen Thanh, M. Bahri, L. Largeau, G. Patriarche, C. Cornet, N. Bertru, A. Le Corre, and O. Durand, J. Appl. Crystallogr. **48**, 702 (2015).
[16]F. Ernst and P. Pirouz, J. Appl. Phys. **64**, 4526 (1988).
[17]T. Quinci, J. Kuyyalil, T. N. Thanh, Y. P. Wang, S. Almosni, A. Létoublon, T. Rohel, K. Tavernier, N. Chevalier, O. Dehaese, N. Boudet, J. F. Bérar, S. Loualiche, J. Even, N. Bertru, A. L. Corre, O. Durand, and C. Cornet, J. Cryst. Growth **380**, 157 (2013).
[18]K. Madiomanana, M. Bahri, J. B. Rodriguez, L. Largeau, L. Cerutti, O. Mauguin, A. Castellano, G. Patriarche, and E. Tournié, J. Cryst. Growth **413**, 17 (2015).
[19]T. J. Grassman, M. R. Brenner, A. M. Carlin, S. Rajagopalan, R. Unocic, R. Dehoff, M. Mills, H. Fraser, and S. A. Ringel, in *34th IEEE Photovoltaic Specialists Conference (PVSC)*, 2009, pp. 002016–002021.
[20]O. Durand, S. Almosni, Y. Ping Wang, C. Cornet, A. Létoublon, C. Robert, C. Levallois, L. Pedesseau, A. Rolland, J. Even, J. M. Jancu, N. Bertru, A. Le Corre, F. Mandorlo, M. Lemiti, P. Rale, L. Lombez, J.-F. Guillemoles, S. Laribi, A. Ponchet, and J. Stodolna, Energy Harvesting Syst. **1**, 147 (2014).
[21]O. Supplie, M. M. May, G. Steinbach, O. Romanyuk, F. Grosse, A. Nägelein, P. Kleinschmidt, S. Brückner, and T. Hannappel, J. Phys. Chem. Lett. **6**, 464 (2015).
[22]A. Beyer, J. Ohlmann, S. Liebich, H. Heim, G. Witte, W. Stolz, and K. Volz, J. Appl. Phys. **111**, 083534 (2012).
[23]W. Kern, J. Electrochem. Soc. **137**, 1887 (1990).
[24]T. Takahagi, I. Nagai, A. Ishitani, H. Kuroda, and Y. Nagasawa, J. Appl. Phys. **64**, 3516 (1988).
[25]F. Chollet, E. André, W. Vandervorst, and M. Caymax, J. Cryst. Growth **157**, 161 (1995).
[26]S. Nayak, D. E. Savage, H.-N. Chu, M. G. Lagally, and T. F. Kuech, J. Cryst. Growth **157**, 168 (1995).
[27]K. Volz, A. Beyer, W. Witte, J. Ohlmann, I. Németh, B. Kunert, and W. Stolz, J. Cryst. Growth **315**, 37 (2011).
[28]V. Narayanan, S. Mahajan, K. J. Bachmann, V. Woods, and N. Dietz, Acta Mater. **50**, 1275 (2002).
[29]A. Beyer, B. Haas, K. I. Gries, K. Werner, M. Luysberg, W. Stolz, and K. Volz, Appl. Phys. Lett. **103**, 032107 (2013).
[30]G. E. Crook, L. Däweritz, and K. Ploog, Phys. Rev. B **42**, 5126 (1990).
[31]J. Zhu, K. Brunner, and G. Abstreiter, Appl. Surf. Sci. **137**, 191 (1999).